

Benchmark Experiment for Photoionized Plasma Emission from Accretion-Powered X-Ray Sources

G. P. Loisel,¹ J. E. Bailey,¹ D. A. Liedahl,² C. J. Fontes,³ T. R. Kallman,⁴ T. Nagayama,¹

S. B. Hansen,¹ G. A. Rochau,¹ R. C. Mancini,⁵ and R. W. Lee⁶

¹*Sandia National Laboratories, Albuquerque, New Mexico 87185, USA*

²*Lawrence Livermore National Laboratory, Livermore, California 94550, USA*

³*Los Alamos National Laboratory, Los Alamos, New Mexico 87545, USA*

⁴*Goddard Space Flight Center NASA, Greenbelt, Maryland 20771, USA*

⁵*University of Nevada, Reno, Nevada 89557, USA*

⁶*University of California, Berkeley, California 94720, USA*

(Received 21 April 2017; published 16 August 2017)

The interpretation of x-ray spectra emerging from x-ray binaries and active galactic nuclei accreted plasmas relies on complex physical models for radiation generation and transport in photoionized plasmas. These models have not been sufficiently experimentally validated. We have developed a highly reproducible benchmark experiment to study spectrum formation from a photoionized silicon plasma in a regime comparable to astrophysical plasmas. Ionization predictions are higher than inferred from measured absorption spectra. Self-emission measured at adjustable column densities tests radiation transport effects, demonstrating that the resonant Auger destruction assumption used to interpret black hole accretion spectra is inaccurate.

DOI: [10.1103/PhysRevLett.119.075001](https://doi.org/10.1103/PhysRevLett.119.075001)

X-ray binaries and active galactic nuclei (AGN) are studied with space telescopes that collect x-ray emission from the accretion-powered plasmas they create [1,2]. The x-ray spectra can be used to infer the nature of the accretor, the accretion rate, and the source luminosity. In the case of black hole accretion, the observed emission constrains the black hole mass and spin [3,4]. Accretion-powered plasmas are photoionized: radiative processes dominate over collisional processes in setting the plasma ionization and state populations [5,6].

Interpreting these observations is challenging because the ionizing source spectrum, its propagation into the plasma, the photoionization kinetics and relevant atomic physics, and finally the emergent intensity as x rays propagate out of the plasma towards the observer all have to be included in the modeling [7,8]. Ultimately, what we learn from accretion-powered objects is impeded by the absence of radiation-driven plasma models benchmarked against accurate laboratory data. In this paper, we describe experiments that for the first time generate highly reproducible emission and absorption spectra, satisfying the requirements to benchmark photoionized plasma models.

Experiments that benchmark photoionization and radiation transport models require production of a large and uniform plasma at astrophysically relevant conditions, with long enough duration for acquiring accurate measurements and reaching steady state, and with an independent thorough plasma conditions characterization. The plasma conditions and spectra need to be measured with high reproducibility, with spectral resolution adequate to test model approximations. Experiments for any plasma type that meet these criteria are rare. However, examples do exist for collisional

plasmas [9–11], providing reproducible data suitable to test radiation properties, with maximum experimental error of 6% in line shape measurements [9] and 10% for spectral transmission measurements [10,11].

There have been no adequate benchmark experiments for photoionized plasma emission until now, in part because ensuring radiation processes dominate over collisions requires a large ratio of the incident irradiance to the electron density. This is difficult to achieve. The irradiance from the largest terrestrial x-ray sources can be comparable to accretion-powered objects, but only for samples placed \leq few cm to the source. This by itself is notable, since accretion-powered objects are among the most luminous celestial sources. However, laboratory densities cannot be too low, because benchmark experiments require high signal-to-noise (S/N) spectra. This depends on the product of the density and the size. One could reduce the density and compensate with increased size, but the plasma size must be smaller than the distance to the source in order to avoid geometrical dilution that causes nonuniformity. These competing requirements can be met only with large facilities that emit copious x rays, efficient spectrometers, and experiment designs that balance the tradeoffs.

Photoionized plasma experiments have been underway at Sandia National Laboratories for more than fifteen years [12–14], providing the foundation for the work described here. These experiments measured absorption spectra that tested photoionized plasma ionization models for the first time [13], but they did not test emission models. Experiments using laser heating have also explored photoionized plasma physics. Some of these measured emission spectra [15], but the short duration required time-dependent

spectral simulations, in contrast to the steady state assumed in astrophysics. Spatial gradients and limited reproducibility further hindered astrophysical model tests [16]. The difficulty involved in testing astrophysical models with transient experiments has also limited the usefulness of x-ray free electron laser photoionized plasma experiments [17]. The situation for astrophysical accretion emission spectroscopy today is that complex spectra are interpreted using models that have not been sufficiently benchmarked against laboratory experiments.

One example of an untested radiation transport hypothesis is the resonant Auger destruction (RAD) [18,19] used to interpret black hole accretion disk emission spectra. Excited L -shell ions (3 to 9 electrons) decay by Auger ionization or $K\alpha$ photon emission. The relatively high Auger probability and the fact that emission from L -shell ions can be resonantly absorbed makes it plausible that the $K\alpha$ emission will be destroyed before it emerges. On the other hand, He-like ions are not affected by Auger ionization and neutral atom emission is not resonantly absorbed. $K\alpha$ emission from L -shell ions was therefore assumed [18,19] to be negligible compared to the He-like or neutral emission. This helped interpret iron $K\alpha$ with a remarkable, several-keV red wing that is believed to be relativistically broadened emission from near the event horizon of a black hole [18–20]. The RAD assumption was used to explain why L -shell ion emission was apparently not observed, even though the accretion disk models include these ions. This assumption was later questioned as L -shell ion lines were observed from Vela X -1 and Cygnus X -3 [21,22] and based on detailed atomic physics modeling [23]. X-ray astronomy has advanced since the RAD approximation was first invoked and the spectra appear to be more complex and varied than was initially appreciated. New models [24,25] are being developed to interpret the spectra without this assumption, although some efforts continue to assume complete RAD destructivity. A goal for the present work is to evaluate the assumption [18,19] that sets $K\alpha$ emission from L -shell ions to 0 because of the RAD mechanism.

Experiment description.—The requirements above are met using an x-ray source [26] driven by 26 MA peak current from Sandia’s Z machine. It generates a 1.6 MJ x-ray burst with an ~ 3 ns full-width-half-maximum (FWHM) and ~ 220 TW peak power. The experiment [Fig. 1(a)] creates a photoionized Si plasma diagnosed with absorption and emission x-ray spectroscopy.

These examine individually three basic processes involved in accretion disk emission modeling: (i) space-resolved emission spectra study transport of the x-ray driving radiation as it propagates into the plasma; (ii) absorption and emission spectra test the understanding of ground and excited state population production within each plasma volume element; and (iii) emission spectra measured from different plasma lengths supply information about transport of the emitted radiation as it propagates out of the plasma.

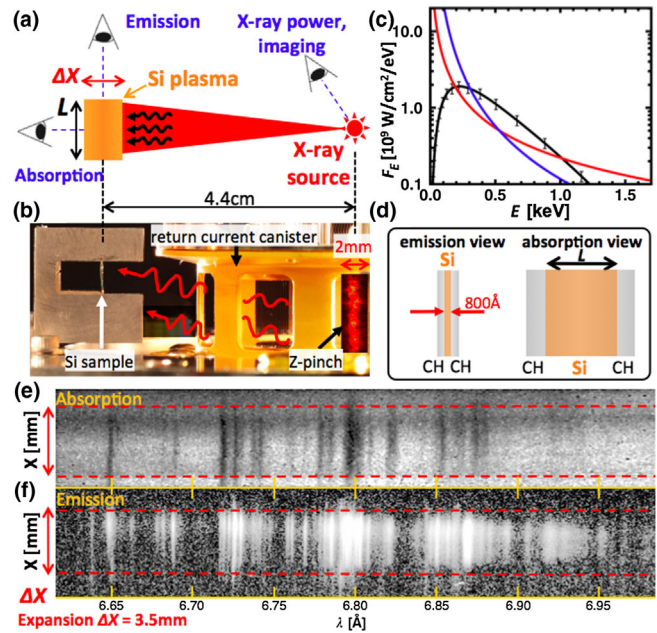


FIG. 1. (a) Top-view schematic: the silicon sample is heated by x ray and expands to low density. X-ray diagnostics characterize the absolute x-ray irradiance on the sample. (b) Side-view photograph showing the Z-pinch radiator and the sample locations. (c) Measured spectral irradiance (black). Overlaid, typical AGN power law spectra with the same Si ionizing flux as the experiment with 1.3 (red) and 2.3 (blue) exponents. (d) The CH-tamped silicon is mounted edge-free enabling self-emission collection, with a 3 mm tall aperture to avoid plasma edges [Fig. 1(b)]. The CH extends 1 mm beyond the Si length $L = 3, 6,$ and 12 mm, preventing lateral expansion. (e) Absorption spectral image (linear scale). (f) Emission image collected at 90° from the absorption line of sight (log scale).

The plasma is made of the astrophysically abundant element silicon ($Z = 14$). The Si is photoionized into the L shell and therefore serves as a surrogate for iron in black hole accretion disks. It is also suited for RAD process studies since Si Auger yields are higher than for Fe. The sample consists of an 800 Å thick Si and O ($O/Si \sim 0.49$) layer tamped on both sides with 1000 Å CH. The CH tamping and the large area-to-thickness ratio promote one-dimensional uniform expansion [27]. The plasma heats and expands under the ~ 110 ns phase when the Z-pinch plasma approaches the axis. The 3.5 mm FWHM expansion size at the final stagnation radiation burst was measured using both space-resolved absorption and emission spectra [Figs. 1(e) and 1(f)]. The $3.1 \times 10^{17} \pm 5\%$ Si/cm² silicon areal density along the axis of expansion is obtained from Rutherford backscattering spectrometry (RBS). Assuming uniform expansion, we obtain $8.5 \pm 1.0 \times 10^{17}$ Si/cm³ density. The 1.5×10^{17} cm⁻² oxygen areal density was also measured with RBS. The electron density (n_e) is inferred from measurements of the Si and O densities and the ionization (see below).

Testing models requires measurements of the spectral irradiance incident on the sample. The absolute source power is measured using silicon diodes and bolometers [28].

However, the sample is bathed in radiation from both the pinch plasma and reemission from the surrounding components [26]. To characterize these sources, we record time-gated monochromatic pinhole images [29] calibrated with the measured power. Then, the spectral irradiance history on the sample located 4.4 cm from the pinch axis was inferred using three-dimensional view factors [30]. The spectrum is non-Planckian [Fig. 1(c), black curve], with $1.6 \times 10^{19} \text{ erg.s}^{-1} \text{ cm}^{-2}$ peak spectrally integrated irradiance.

The photoionization parameter $\xi = 4\pi F/n_e$ characterizes photoionized plasmas [5,6], with F the spectrally integrated flux. This places work in context, but is limited because the ionization depends on the incident spectrum and the plasma composition. If, as in prior laboratory work, we use the measured n_e and the irradiance above $\sim 167 \text{ eV}$ photon energy capable of ionizing Si, we find $\xi \sim 20 \text{ erg.cm.s}^{-1}$. However, accretion-powered plasmas typically involve a power law incident spectrum [e.g., Fig. 1(c), red and blue spectra] and the dominant element is hydrogen. Power law spectra scaled such that the flux capable of ionizing Si is the same as in the experiment include a surplus of low energy photons. These ionize hydrogen but not Si. Therefore, astrophysical ξ values with the same Si ionization as in the experiment are approximately $\xi \sim 20\text{--}300 \text{ erg.cm.s}^{-1}$, depending on the power law index. This definition [6] relates laboratory conditions to astrophysical plasmas, but model tests must use the measured spectral irradiance.

Absorption spectroscopy.—The pinch stagnation emission backlights the expanded silicon plasma and a slit-imaging high-resolution ($\lambda/\delta\lambda \sim 2400$) spectrometer records absorption spectra. The time-integrated instrument averages over the 3 ns FWHM backlight. The transmitted spectrum, dispersed by a convex thallium acid phthalate crystal used in second order, is recorded on x-ray film. Averaging over 16 spectra acquired by two spectrometers in eight experiments reduced the errors and the 4.8% spectrum-average standard deviation confirmed reproducibility (Fig. 2).

Transitions from different charge states (Fig. 2) can be used to infer the charge state distribution [13,14,31]. In photoionized plasmas the charge state distribution is mostly determined by the driving radiation. Yet, for $T_e \sim 10\text{--}15 \text{ eV}$ electron temperatures, the Li-like (Si^{+11}) ground state $1s^2 2s$ and the low-lying $1s^2 2p$ state are predicted to reach partial local thermodynamic equilibrium and their relative populations depend mostly on T_e . We infer $T_e = 33 \pm 7 \text{ eV}$ using line ratios from these states (Fig. 2). At $T_e = 33 \text{ eV}$, the dominant charge state in a collision-dominated silicon plasma is Si^{+5} (F -like). The observed higher ionization demonstrates that the plasma here is effectively photoionized.

The column densities ($\sim 1\text{--}10 \times 10^{17} \text{ Si/cm}^2$) and photoionization parameters ($\xi \sim 20\text{--}300 \text{ erg.cm.s}^{-1}$) are similar to typical accretion disk conditions. Most accretion powered plasmas are believed to have notably lower n_e , although some

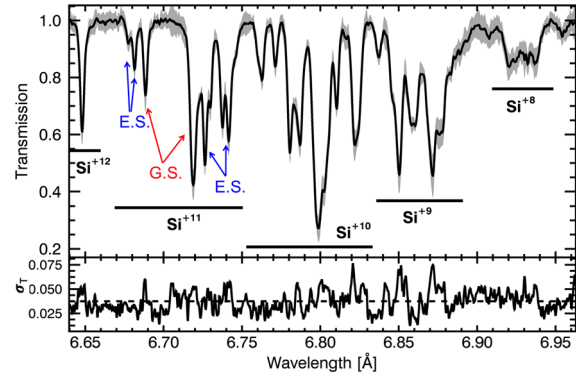


FIG. 2. Measured $1s\text{--}2p$ $K\alpha$ silicon plasma transmission spectrum. Top: Mean over 16 measurements with the standard deviation shown as grey background. Lines arising from Li-like (Si^{+11}) $1s^2 2s$ ground state (G.S.) and $1s^2 2p$ singly excited state (E.S.) used to infer electron temperature are indicated. Bottom: Absolute standard deviation in the mean transmission, with spectral mean (dashed).

recent studies infer n_e values comparable to the experiment [24]. Nevertheless, the results provide valuable tests even for much lower n_e as long as collisional processes are relatively unimportant compared to the radiative process. Calculations predict that photoionization is more important than collisional ionization for the conditions considered here. Furthermore, radiative and dielectronic recombination rate predictions are comparable to or greater than three-body recombination. However, these estimates depend on both the energy levels and ionization states under consideration, as well as the models themselves that are the subject of the present tests. Thus, extrapolation of the present results to lower densities requires care.

The absorption data test photoionized plasma model for plasma ionization and energy level populations that arise. Here, we restrict our investigation to the question of whether models using the measured non-Planckian spectral irradiance [Fig. 1(c), black curve], T_e , and n_e as inputs can successfully predict the ionization and populations that produce the absorption spectra. We find that the ATOMIC [32] and XSTAR [33] models disagree with the observed transmission. Both overpredict the ionization, with $\bar{Z} \sim 11$ (Fig. 3, top). The origin of this discrepancy is presently unknown. Lowering the drive irradiance within the measurement uncertainty lowers the predicted ionization, but does not resolve the discrepancy. A possible concern is that the XSTAR and ATOMIC models here assumed steady state and the plasma duration is comparable to the time needed to reach steady-state populations. However, calculations with the SPECT3D [34] model including transient kinetic effects showed that these effects were small compared to the differences displayed in Fig. 3. Reasonable transmission agreement can be obtained if the input parameters are adjusted to favor more recombination, such that $\bar{Z} \sim 10$ (Fig. 3, bottom). This could result if the true recombination rates are higher than in the models, or if the true n_e is two to

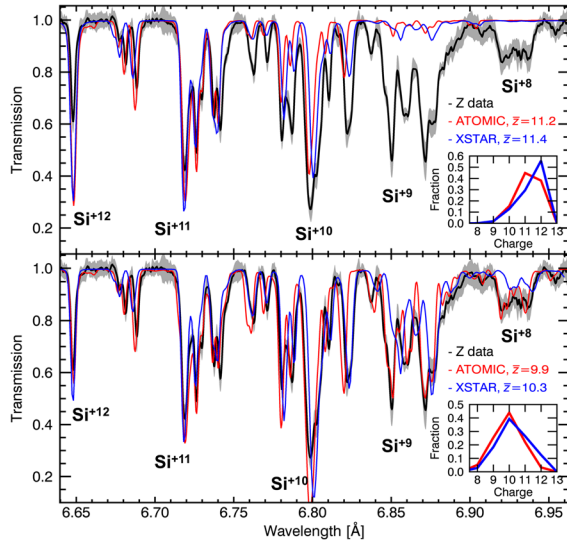


FIG. 3. Transmission compared with ATOMIC and XSTAR models. Top: Models predict an overionized transmission at experimentally inferred conditions. Bottom: Tested models give reasonable agreement when $\bar{Z} \sim 10$, with adjusted conditions of $T_e = 25$ eV and $2\times$ density, $n_e = 1.7 \times 10^{19}$ cm $^{-3}$, for ATOMIC, and with $4\times$ density, i.e., $T_e = 33$ eV, $n_e = 3.4 \times 10^{19}$ cm $^{-3}$ for XSTAR. On each panel the charge state distributions for each calculation are shown in the inset.

four times higher than the measured value. The latter possibility is inconsistent with the estimated density error.

Emission spectroscopy.—A major difficulty for emission measurements is the harsh experiment environment. The Z-pinch radiation is $\sim 10^7$ times brighter than the Si emission and the discharge produces high energy background x rays, mechanical shock, and plasma debris that can ruin data and destroy spectrometer crystals. This was overcome using a concave spherical crystal (quartz 10-10) spectrometer in the FSSR-1D [35] configuration, achieving high sensitivity (<0.25 [1.85 keV]-photon/ μm^2 on detector) and high spectral resolution ($\lambda/\delta\lambda = 2800\text{--}4400$).

The silicon emission is recorded at 90° to the sample normal, along the variable length L [Fig. 4; also see Fig. 1(d)]. The emission measurements at 2.5 , 5 , and 10×10^{17} Si/cm 2 column densities have 5.7%, 5.2%, and 11.2% mean standard deviations for the $L = 3$, 6, and 12 mm lengths, respectively. This demonstrates good reproducibility.

The emission and absorption spectra arise from the same instant in the plasma evolution since they are both created by $h\nu \geq 1800$ eV photons emitted at peak drive. Emission depends on the K -shell vacancy creation while absorption depends on bound-bound transitions in that photon energy range. Thus, the results can be employed simultaneously to obtain the strongest possible future model constraints. Work is in progress to improve the constraints with an absolute spectral radiance calibration and by confirming the applicability of the relative spectral response calibration used here [36].

The emission data presented here are space-integrated lineouts taken from space-resolved spectral images [Fig. 1(f)]. The plasma is optically thin to higher energy photons that photoionize the Si K shell, but optically thick to the resonant photons that cause photoexcitation. Thus, future studies of the space-resolved data could help build better understanding of the population processes that lead to $K\alpha$ emission.

Emission modeling is in progress and detailed model comparisons are beyond the scope of this article. Nevertheless, the measurements show that if the He α is observed and L -shell ions are present, then the L -shell ion lines should also be observed. The Si column densities in this experiment and the corresponding optical depths are similar to relevant astrophysical plasmas. Thus, completely destructive RAD is not an accurate approximation.

The optical depths for the lines observed here are between 0.2 and 60 at line center. The thinnest lines originate from throughout the plasma and the thicker lines preferentially originate from the periphery, just as they would for astrophysical plasmas with similar depths. The brightest L -shell lines have 5 to 15 optical depths for the 3 mm case, meaning those lines undergo many absorption-reemission events. Therefore, the experiment satisfies the

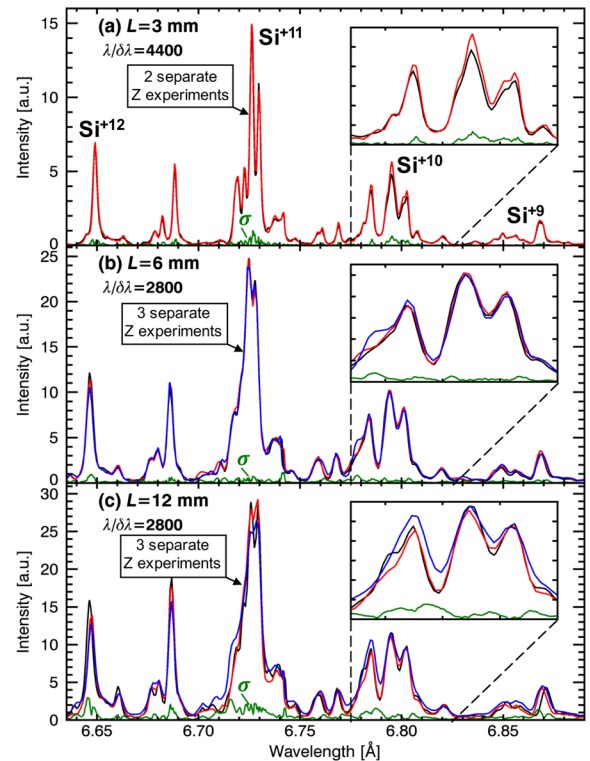


FIG. 4. Silicon emission collected for three column densities (contributing ions are labelled in top panel). Intensity units are proportional to $J \cdot \text{\AA}^{-1} \cdot \text{sr}^{-1} \cdot \text{cm}^{-2}$. The observed column density is adjusted with the variable length $L = 3$ mm (a), 6 mm (b) and 12 mm (c). The standard deviation σ (green curves) and resolving power are given in each plot. The enlarged plot segments (insets) further illustrate the reproducibility.

component of the original RAD assumption that the plasma should have optically thick L -shell ion lines. A possible question is whether velocity gradients in the plasma might broaden the lines sufficiently to reduce the line center optical depths enough to make the probability of absorption less than 1. In order to investigate this, we performed measurements with even higher spectral resolution ($\lambda/\delta\lambda \sim 9200$). These measurements, not presented here, set an $\sim 30 \mu\text{m}/\text{ns}$ upper bound on the plasma velocities. The velocity-distribution-induced shifts are convolved with the optical depth to obtain the optical depth modified by the plasma motion. This reduces the line center optical depth slightly, but it is still above 5 for most lines. The smallness of the measured velocity gradients supports the conclusion regarding RAD.

This raises the following question: What processes are responsible for the apparent absence of L -shell ion $K\alpha$ emission in some AGN emission spectra? The present experiment can help solve this problem. If models can be refined to predict the measured emission and absorption self-consistently, then we can evaluate how the RAD mechanism quenches specific lines and to what degree. These results offer an extensive test for recently developed models that do not employ the RAD hypothesis. Such benchmarked models may then help refine the AGN observation interpretations.

The authors are grateful to the entire team at the Z facility. We especially acknowledge Dr. E. Harding for his assistance in developing the emission spectrometer and Dr. A. Wootton and Dr. R. Falcon in reviewing the manuscript. Sandia National Laboratories is a multi-mission laboratory managed and operated by National Technology and Engineering Solutions of Sandia, LLC., a wholly owned subsidiary of Honeywell International, Inc., for the U.S. Department of Energy's National Nuclear Security Administration under Contract No. DE-NA-0003525.

-
- [1] A. Kinkhabwala, M. Sako, E. Behar, S. M. Kahn, F. Paerels, A. C. Brinkman, J. S. Kaastra, M. F. Gu, and D. A. Liedahl, *Astrophys. J.* **575**, 732 (2002).
 - [2] T. Kallman, D. A. Evans, H. Marshall, C. Canizares, A. Longinotti, M. Nowak, and N. Schulz, *Astrophys. J.* **780**, 121 (2014).
 - [3] Y. Tanaka, K. Nandra, A. C. Fabian *et al.*, *Nature (London)* **375**, 659 (1995).
 - [4] C. S. Reynolds, *Space Sci. Rev.* **183**, 277 (2014).
 - [5] C. B. Tarter, W. H. Tucker, and E. E. Salpeter, *Astrophys. J.* **156**, 943 (1969).
 - [6] D. A. Liedahl, *Astrophys. Space Sci.* **336**, 251 (2011).
 - [7] C. W. Mauche, D. A. Liedahl, B. F. Mathiesen, M. A. Jimenez-Garate, and J. C. Raymond, *Astrophys. J. Lett.* **606**, 168, (2004).
 - [8] J. García and T. R. Kallman, *Astrophys. J.* **718**, 695 (2010).
 - [9] W. L. Wiese, D. E. Kelleher, and D. R. Paquette, *Phys. Rev. A* **6**, 1132 (1972).

- [10] J. E. Bailey, G. A. Rochau, C. A. Iglesias, J. Abdallah, Jr. *et al.*, *Phys. Rev. Lett.* **99**, 265002 (2007).
- [11] J. E. Bailey, T. Nagayama, G. P. Loisel, G. A. Rochau, *et al.* *Nature (London)* **517**, 56 (2015).
- [12] J. E. Bailey, D. Cohen, G. A. Chandler, M. E. Cuneo, M. E. Foord, R. F. Heeter *et al.*, *JQSRT* **71**, 157 (2001).
- [13] M. E. Foord *et al.*, *Phys. Rev. Lett.* **93**, 055002 (2004).
- [14] I. M. Hall, T. Durmaz, R. C. Mancini, J. E. Bailey, G. A. Rochau, I. E. Golovkin, and J. J. MacFarlane, *Phys. Plasmas* **21**, 031203 (2014).
- [15] S. Fujioka, H. Takabe, N. Yamamoto, D. Salzmann *et al.*, *Nat. Phys.* **5**, 821 (2009).
- [16] E. Hill and S. Rose, *Phys. Plasmas* **17**, 103301 (2010).
- [17] L. Young, E. P. Kanter, B. Krässig, Y. Li *et al.* *Nature (London)* **466**, 56 (2010).
- [18] R. R. Ross and A. C. Fabian, *Mon. Not. R. Astron. Soc.* **261**, 74 (1993).
- [19] R. R. Ross, A. C. Fabian, and W. N. Brandt, *Mon. Not. R. Astron. Soc.* **278**, 1082 (1996).
- [20] A. C. Fabian, A. Zoghbi *et al.*, *Nature (London)* **459**, 540 (2009).
- [21] M. Sako, D. A. Liedahl, S. M. Kahn, and F. Paerels, *Astrophys. J.* **525**, 921 (1999).
- [22] S. Watanabe, M. Sako, M. Ishida, Y. Ishisaki, S. M. Kahn, T. Kohmura, F. Nagase, F. Paerels, and T. Takahashi, *Astrophys. J.* **651**, 421 (2006).
- [23] D. A. Liedahl and G. V. Brown, *Can. J. Phys.* **86**, 183 (2008).
- [24] J. A. García, A. C. Fabian, T. R. Kallman, T. Dauser, M. L. Parker, J. E. McClintock, J. F. Steiner, and J. Wilms, *Mon. Not. R. Astron. Soc.* **462**, 751 (2016).
- [25] B. E. Kinch, J. D. Schnittman, T. R. Kallman, and J. H. Krolik, *Astrophys. J.* **826**, 52 (2016).
- [26] G. A. Rochau, J. E. Bailey, R. E. Falcon, G. P. Loisel, T. Nagayama, R. C. Mancini, I. Hall, D. E. Winget, M. H. Montgomery, and D. A. Liedahl, *Phys. Plasmas* **21**, 056308 (2014).
- [27] T. Nagayama, J. E. Bailey, G. Loisel, G. A. Rochau, J. J. MacFarlane, and I. Golovkin, *Phys. Rev. E* **93**, 023202 (2016).
- [28] M. C. Jones, D. J. Ampleford, M. E. Cuneo, R. Hohlfelder *et al.* *Rev. Sci. Instrum.* **85**, 083501 (2014).
- [29] B. Jones, C. Deeney, C. A. Coverdale, C. J. Meyer, and P. D. LePell, *Rev. Sci. Instrum.* **77**, 10E316 (2006).
- [30] J. J. MacFarlane, *JQSRT* **81**, 287 (2003).
- [31] E. Behar and H. Netzer, *Astrophys. J.*, **570**, 165 (2002).
- [32] C. J. Fontes, H. L. Zhang, J. Abdallah, Jr., R. E. H. Clark, D. P. Kilcrease, J. Colgan, R. T. Cunningham, P. Hakei, N. H. Magee, and M. E. Sherrill, *J. Phys. B* **48**, 144014 (2015).
- [33] T. Kallman and M. Bautista, *Astrophys. J. Suppl. Ser.* **133**, 221 (2001).
- [34] J. J. MacFarlane, I. E. Golovkin, P. Wang, P. R. Woodruff, and N. A. Pereyra, *High Energy Density Phys.* **3**, 181 (2007).
- [35] E. C. Harding, T. Ao, J. E. Bailey, G. Loisel, D. B. Sinars, M. Geissel, G. A. Rochau, and I. C. Smith, *Rev. Sci. Instrum.* **86**, 043504 (2015).
- [36] G. Hölzer, O. Wehrhan, and E. Förster, *Cryst. Res. Technol.* **33**, 4 (1998).